Communication

Microstructures and Mechanical Properties of *In Situ* Al_2O_3/Al-Si Composites Fabricated by Reaction Hot Pressing

EL OUALID MOKHNACHE, G.S. WANG, L. GENG, and L.J. HUANG

Three *in situ* formed Al_2O_3/Al-Si composites with a different volume fraction of 10, 20, and 30 vol pct were fabricated using low energy ball milling and reaction hot pressing. The effect of reinforcement volume fraction on the microstructure and mechanical properties were studied. When the volume fraction was 30 vol pct, a massive primary Si (~130 μm) along with an increase of Al_2O_3 (~2 μm) was observed. The YS, UTS, and Brinell hardness of the composites were significantly higher than the aluminum matrix. Mechanisms governing the tensile fracture process are discussed.

DOI: 10.1007/s11663-014-0203-z

Recently, aluminum matrix composites (AMCs) have been used widely as potential materials in many areas such as automobile, aerospace, and military applications. Moreover, their attractive mechanical and thermal properties including density *vs* strength, low thermal expansion, wear resistance, and resistance to elevated temperature make AMCs an excellent overcoming means to many technology progresses.[1–4] Reactive hot pressing (RHP) has been suggested to overcome the high concentration of porosity, which occurs during the *in situ* processing of composites. There, the *in situ* reinforcements are synthesized by an exothermic conversion of the reactants, followed by hot compaction to obtain near fully dense composites.[5,6] It has been reported that after the aluminum melts, the reduction of silica takes place forming Al_2O_3 and Si.[7] Based on the following reaction, the *in situ* Al_2O_3/Al-Si composite can be synthesized as following:

$$3SiO_2 + 4Al \rightarrow 2Al_2O_3 + 3Si \quad [1]$$

In this work, for the first time RHP was employed to fabricate Al_2O_3/Al-Si composites. Moreover, no reported works were carried out to clarify the effect of volume fraction of reinforcement in Al-SiO_2 system. Three composites reinforced with 10, 20, and 30 vol pct were fabricated by RHP, with the aim to investigate the effect of volume fraction of reinforcement on microstructure and tensile properties at room temperature. The tensile fracture mechanisms were also studied.

Pure Al powders (99.6 pct purity) and SiO_2 powders (99.2 pct purity), with an average size of 30 and 2 μm, respectively, were used as raw materials. To produce, the *in situ* composites namely M10, M20, and M30 with different volume fractions 10 pct (*i.e.*, 7.1 vol pct Al_2O_3 + 2.9 vol pct Si + 90 vol pct Al), 20 pct (*i.e.*, 14.2 vol pct Al_2O_3 + 5.8 vol pct Si + 80 vol pct Al), and 30 pct (*i.e.*, 21.3 vol pct Al_2O_3 + 8.7 vol pct Si + 70 vol pct Al) respectively, the stoichiometric starting materials were weighed according to the hypothetical Reaction [1]. The powder mixtures were ball milled using low energy at 160 rpm for 4 hours in a planetary ball mill under an argon atmosphere with a milled media to material ratio of 4:1. The mixture powders were transferred into the graphic mold pre-coated with boron nitride to avoid the reaction between the mold and the reactants. In a vacuum of 4.5×10^{-2} Pa, different stages were used to fabricate the composites, at the first stage, the powders were heated to 873 K (600 °C) and compacted with 25 MPa for 1 hour, at the second stage, the compact was heated to the synthesis temperature [1173 K (900 °C)] for 1 hour to complete the reaction. At the final stage, the compact was cooled down to 853 K (580 °C) and re-compacted with 25 MPa for 1 hour to produce dense composites. Hydrostatic weighing method was used to measure the relative density of the samples. Scanning electron microscopic (SEM, Quanta 200FEG) and transmission electron microscopy (TEM, TECNAIF30) along with energy dispersive X-ray spectroscopy (EDX) were used to investigate the microstructure and morphology of the composites. Brinell hardness measurements were carried out on samples using HB-3000B-1 machine with load force of 9807 N and indenter ball diameter of 5 mm for dwell time of 30 seconds. Room temperature tensile tests, which refer to the metal materials testing standards of ISO 6892: 1998,[8] were carried out using an Instron-5569 universal testing machine at a constant crosshead speed of 0.5 mm/min. A total of three tensile samples with gage dimensions of 15 mm × 5 mm × 2 mm were tested for each material.

According to Breslin *et al.*,[7] the Reaction [1] forming Al_2O_3 and Si is exothermic and spontaneous at the experiment temperature [1173 K (900 °C)]. Therefore, XRD plots as seen in Figure 1 revealed that all the composites mainly constituted three phases, namely Al_2O_3, Si, and Al. Also, no un-reacted SiO_2 was detected which indicates that the reduction of silica occurred completely with the employed synthesis temperature and holding time.

In Al-Si binary system,[9] three regions can be distinguished as the content of Si increases. These are the hypoeutectic (less than 12.6 wt pct of Si), eutectic (≈12.6 wt pct of Si), and hypereutectic (more than 12.6 wt pct of Si). Using a reinforcement fraction of

EL OUALID MOKHNACHE, Doctor Candidate, G.S. WANG and L.J. HUANG, Associate Professors, and L. GENG, Professor, are with the School of Materials Science and Engineering, Harbin Institute of Technology, Harbin 150001, P.R. China. Contact e-mail: wangguisong@hit.edu.cn

Manuscript submitted March 9, 2014.
Article published online October 10, 2014.

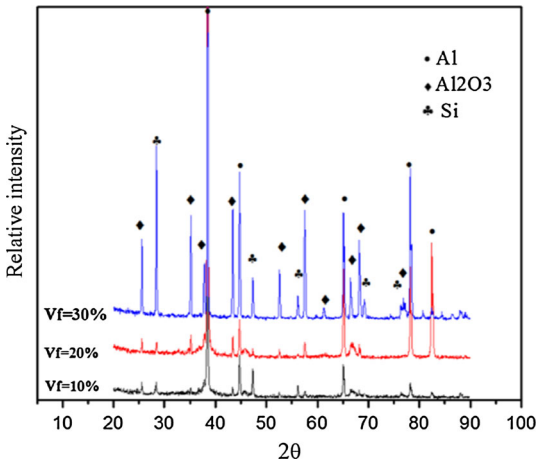

Fig. 1—X-ray analysis of composites.

10, 20, and 30 vol pct, a mass of approximately 3.2, 8.1, and 13.1 wt pct of Si are expected to be formed, respectively. Therefore, the *in situ* composites obviously have quite different morphologies with increasing volume fraction of reinforcement as shown in Figure 2.

Composites M10 and M20 as shown in Figures 2(a) and (b) confirm the presence of the *in situ* synthesized Al_2O_3 (dark gray color) and Si (light gray color) particles dispersed in Al matrix, and their sizes were found less than 2 μm. Otherwise, the Si would dissolve in Al to form the hypoeutectic Al-Si as new matrix. In the case of composite M30, Figure 2(c) shows that more Al_2O_3 was produced, as compared to composites M10 and M20, and massive Si blocks with a size of around 130 μm were observed. SEM with EDS result of composite M30, as seen in Figures 2(d) and (e), revealed that these blocks constitute 100 wt pct Si (EDS result of point (A) in Figures 2(d)). This indicates that the primary silicon is formed and the hypereutectic Al-Si exists as a new matrix for the composite M30. Furthermore, Figure 2(f) confirms the presence of Al_2O_3 (EDS result of point (B) in Figure 2(d)) comprising O (36.34 wt pct) and Al (63.66 wt pct).

TEM, diffraction pattern and EDX of composite M10, as shown in Figure 2(g), clearly show that Al_2O_3 (rhombohedral) and Si (cubic) were dispersed in Al forming a clean interface. Al_2O_3 and Si had polygonal shape with a size of around 1.2 and 0.3 μm, respectively. The presence of twins in silicon can be attributed to its growth during cooling.

From Table I, it can be seen that the increase of the volume fraction of reinforcement has led to a significant increase of hardness, as compared to Al matrix. This increment can be attributed to the formation of Al_2O_3 and Si as hardening phases. Moreover, by comparing the composite M20 with M10, the yield strength and ultimate tensile strength were increased from 59, 121 to 153, 237 MPa, respectively, with a decrease of ductility from 12.4 pct to 6.7 pct. In the case of M30, despite the employed reinforcement fraction of 30 vol pct, a further decrease of UTS and ductility with a slight increase of yield strength was observed. Furthermore, it can be seen that the relative density of the composite M30 decreased when a high volume fraction was used, resulting in the degradation of its mechanical properties.

It is worth mentioning that, the mechanical properties of Al-Si cast alloys depend on several microstructural parameters. Grain size, secondary dendrite arm spacing, distribution of phases, the presence of secondary phases or inter-metallic compounds, the morphology of silicon particles (size, shape and distribution) and, finally, defects play a key role in the determination of the elastic and plastic behavior of aluminum alloys.[10–13] From all of these aspects, mechanical properties of some hypo/hyper Al-Si alloys and the fabricated composites are summarized and compared, as shown in Table I. When compared with the Al-Si alloys in References 13 and 14, composite M20 contained approximately the same amount of Si (8.1 wt pct), but demonstrated a significant increase in YS (69.98, 44.61 pct) and UTS (21.27, 20.42 pct). Moreover, in comparison with the Al-9wt pct Si, composite M20 showed an improvement in YS (94 MPa) and UTS (171 MPa) with similar elongation (6.7 pct). This improvement in tensile properties of the composite M20 is attributed to the *in situ* generated Al_2O_3 in M20 composite. However, when compared with the sand-cast unmodified Al-12wt pct Si,[15] composite M30, which almost contained the same weight content of Si, demonstrated a decrease in YS, UTS, and elongation of 17.64, 30.69, and 98.75 pct, respectively. The increased presence of Al_2O_3, in the case of M30, led to a degradation of its tensile properties when compared with the Al-Si alloy. On one hand, this degradation can be attributed to the formation of large pores due to the increased volume fraction of reinforcement. The same information was reported by Gupta *et al.*,[13] it was found that the increase of Si content in Al-Si alloy from 10 to 19 wt pct, led to a decrease of tensile properties. On the other hand, as shown in Figure 2(d), the embedded Al_2O_3 in the large massive silicon might also have played a key role on this degradation, where a poor interfacial bonding between Al_2O_3 and primary Si is formed.

Tensile fracture surfaces of the composites M10, M20, and M30 are shown in Figure 3. It can be seen that the fracture surface of composite M10 (Figures 3(a) and (b)) is composed of fine dimples with Al_2O_3 particles pulled out, suggesting that the composite M10 had a good ductility (≈12.4 pct). Therefore, the composite M10 underwent a ductile fracture.

In the case with M20, the usage of 20 vol pct has led to the increase of Al_2O_3 and Si contents. The high content of Al_2O_3 can contribute to enhance the strength of the composite by Orowan strengthening mechanism.[16,17] The Al_2O_3 particle behaves as an obstacle to slow the movement of dislocation, thereby the dislocation passes through Al_2O_3 as shown in Figure 3(c). This indicates that a good interface bonding between Al_2O_3 and Al is formed. The presence of the brittle Si is regarded as favorite location for the crack initiation. Consequently, the fracture characteristic of the Al_2O_3/Al-Si composite is more brittle in nature. Moreover, in Al-Si alloys the tensile properties are mainly affected by the size and morphology of the hard and brittle silicon precipitates,[13] which is the case of the

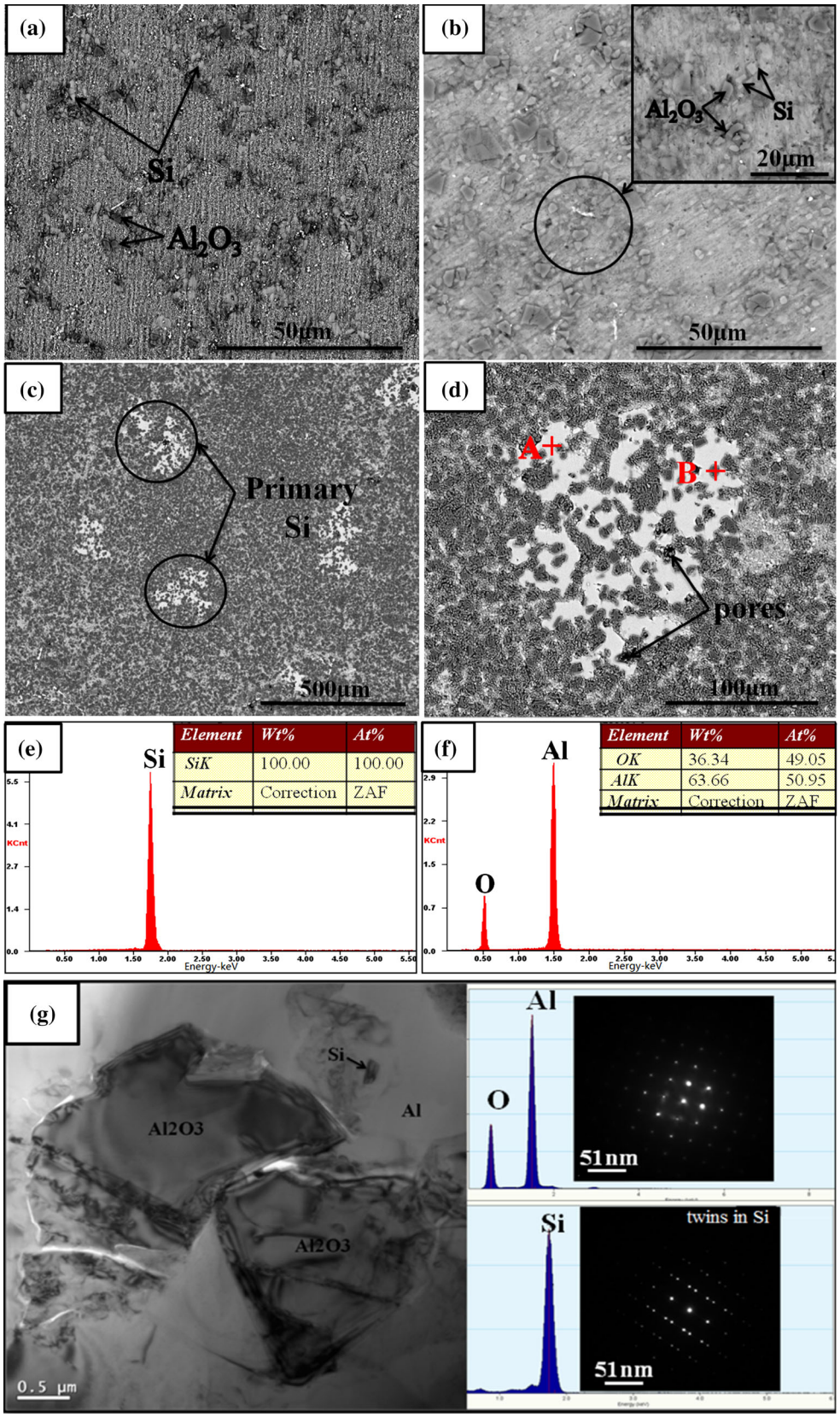

Fig. 2—SEM of composites (*a*) M10, (*b*) M20, (*c*) M30. (*d*) SEM along with EDS result of composite M30, (*e*) EDS result of point A in (d). (*f*) EDS result of point B in (d) and (*g*) TEM image, diffraction pattern, and EDX showing the polygonal Al_2O_3 (rhombohedral) and Si (cubic) particles.

Table I. Material Nomenclature with Corresponding Mechanical Properties

Composites (M_{Vf})	Yield Strength YS (MPa)	Ultimate Tensile Strength UTS (MPa)	Hardness	Elongation (pct)	Relative Density
M10	59 ± 2	121 ± 2	45 ± 0.1 (HB)	12.4 ± 0.15	98.9 pct
M20	94 ± 2	171 ± 3	57 ± 0.3(HB)	6.7 ± 0.2	98.7 pct
M30	98 ± 3	107 ± 2	82 ± 0.1(HB)	0.14 ± 0.3	96.6 pct
Al-7 wt pct Si[13]	55.3	141.7	—	12.2	—
Al-9 wt pct Si[14]	65	142	72 (HV)	8	—
Al-10 wt pct Si[13]	75.46	154.7	—	10.3	—
Al-12 wt pct Si[15]	119	154.5	37 (HRC)	3.2	—
Al-19 wt pct Si[13]	80.86	129.66	43.4 (HV)	2.36	—

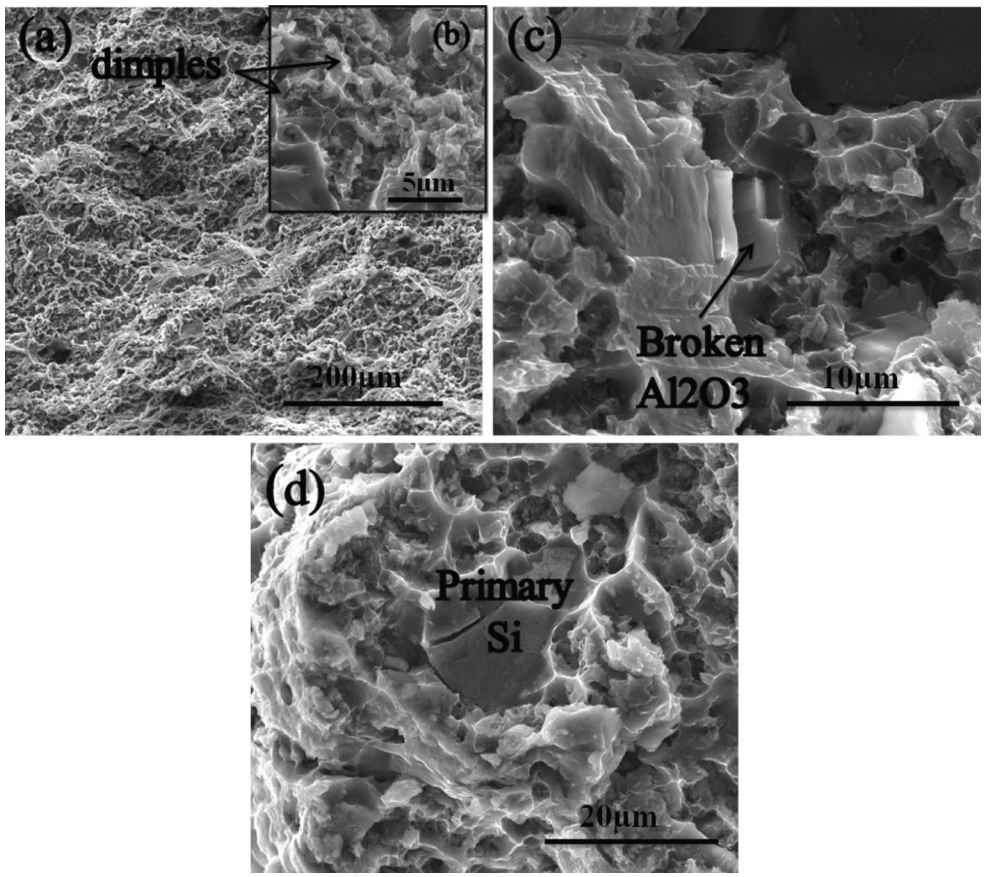

Fig. 3—Tensile fracture surfaces of the composites (*a*) M10 at low and (*b*) high magnification, (*c*) M20 (Orowan strengthening mechanism), and (*d*) M30.

Al_2O_3/Al-Si composite in this study. Furthermore, the presence of the massive primary Si in the composite M30 has harmful effect on the ultimate strength, with a significant decrease in ductility indicating that the composite M30 underwent a brittle fracture (Figure 3(c)).Consequently, the fracture mechanisms of the *in situ* Al_2O_3/Al-Si composite have changed from a ductile fracture to a brittle fracture with increasing volume of reinforcement.

In situ Al_2O_3/Al-Si composites were successfully synthesized from Al-SiO_2 system by RHP with good mechanical properties, as compared to the pure aluminum. Moreover, as the volume fraction of reinforcement increased from 10 to 20 vol pct, an increase of the yield strength and UTS with a decrease of ductility was achieved. However, using 30 vol pct may lead to a further decrease of UTS as well as a significant decrease of ductility. The mechanisms governing the tensile fracture of the *in situ* Al_2O_3/Al-Si composites can be explained by the void nucleation and growth followed by crack initiation from the predominantly brittle Si phase at the interface with Al matrix. Therefore, the

damage of the composite is mainly attributed to the silicon Si content and morphologies of its brittle phase.

This work is financially supported by the National Natural Foundation of China. (Project No.: 51201047).

REFERENCES

1. S.V. Prasad and R. Asthana: *Tribol. Lett.*, 2004, vol. 17, pp. 445–53.
2. W. Speer and O.S. Es-Said: *Eng. Fail. Anal.*, 2004, vol. 11, pp. 895–902.
3. E.S.C. Chin: *Mater. Sci. Eng. A*, 1999, vol. 259, pp. 155–61.
4. J. Eliasson and R. Sandström: *Key Eng. Mater.*, 1995, vol. 104, pp. 3–36.
5. J.J. Moore and H.J. Feng: *Prog. Mater Sci.*, 1995, vol. 39, pp. 243–73.
6. D. Roy, S. Ghosh, A. Basumallick, and B. Basu: *J. Alloys Compd.*, 2007, vol. 436, pp. 111–27.
7. M.C. Breslin, J. Ringlanda, J. Segeer, A.L. Marasco, G.S. Daehn, and H.L. Fraser: *Ceram. Eng. Sci. Proc.*, 1994, vol. 15, pp. 104–12.
8. ISO 6892: Metallic Materials-Tensile Testing at Ambient Temperature, 1998.
9. J.L. Murray and A.J. McAlister: *ASM Handbook Volume 3: Alloy Phase Diagrams*, vol. 15, ASM International, Materials Park, 1992, p. 312.
10. S.G. Shabestary and F. Shahri: *J. Mater. Sci.*, 2004, vol. 39, pp. 2023–32.
11. S. Viswanathan, A.J. Duncan, A.S. Sabau, Q. Han, W.D. Porter, and B.W. Riemer: *AFS Trans.*, 1998, vol. 106, pp. 411–17.
12. V. Rontó and A. Roósz: *Int. J. Cast Met. Res.*, 2001, vol. 13, pp. 337–42.
13. M. Gupta and S. Ling: *J. Alloys Compd.*, 1999, vol. 287, pp. 284–94.
14. W.R. Osório, N. Cheung, L.C. Peixoto, and A. Garcia: *Int. J. Electrochem. Sci.*, 2009, vol. 4, pp. 820–31.
15. C.W. Onyia, B.A. Okorie, I.S. Neife, and C.S. Obayi: *World. J. Eng. Technol.*, 2013, vol. 1, pp. 9–16.
16. R.J. Arsenault: *Mater. Sci. Eng.*, 1984, vol. 64, p. 171.
17. E. Orowan: *Symposium on Internal Stress in Metals and Alloys*, Institute of Metals, 1948, p. 451.